Impact of the hybrid electric architecture on the performance and emissions of a delivery truck with a Dual-Fuel RCCI Engine

Antonio García[a], Javier Monsalve-Serrano[*,a], Santiago Martinez-Boggio[a], Patrick Gaillard[b]

[a]CMT - Motores Térmicos, Universitat Politècnica de València, Camino de Vera s/n, 46022 Valencia, Spain
[b]Aramco Fuel Research Center, Aramco Overseas Company B.V. Paris, France

Applied Energy
Volume 301, 1 November 2021, 117494
https://doi.org/10.1016/j.apenergy.2021.117494

Corresponding author (*):
Dr. Javier Monsalve-Serrano (jamonse1@mot.upv.es)
Phone: +34 963876559
Fax: +34 963876559

Abstract

Reactivity controlled compression ignition combustion showed great advantages in terms of NOx and soot emissions reduction, leading to virtually zero emissions. However, the average brake thermal efficiency of this concept is like that found with conventional diesel operation. The powertrain electrification using electric motors and battery packages appears as a potential solution to reduce the CO_2 emissions. For this reason, several solutions for the powertrain electrification can be found currently in the market as the parallel, series and power split powertrain architectures. The aim of this work is to evaluate the hybrid architecture impact on the fuel consumption and emissions of a delivery truck (Volvo-FL) intended for urban and urban-rural applications. The truck equipped with a reactivity-controlled compression ignition diesel-gasoline engine is evaluated and compared against the conventional diesel case. In addition, to evaluate the impact of new e-fuels on the well-to-wheel CO_2 emissions, a synthetic gasoline coming from carbon capture and green electricity is evaluated. The results show that hybridization allows reducing the tank-to-wheel CO_2 emissions above 15% with the parallel hybrid set-up. The series and power split architectures show CO_2 benefits of 12% with respect to the baseline diesel non-hybrid case. Using synthetic gasoline as low reactivity fuel allows to achieve a 50% well-to-wheel CO_2 reduction in the P2 and 70% well-to-wheel CO_2 reduction for the series and power split cases due to the higher average gasoline fraction used in the driving cycle.

Keywords

E-Components, Mild Hybrid, Dual-Fuel, Emissions Regulations, Driving Cycles

1. Introduction

Pollution in urban and suburban centres has increased throughout the world in the recent years due to an increase in the population and more flexible measures in the transport emissions legislation [1]. Several cities are beginning to ban vehicle without electrification (propelled by internal combustion engines) and in some cases with special attention to diesel-type engines. The NOx and particle matter emissions of Diesel engines have been put into discussion after the Dieselgate [2]. However, compression ignition (CI) engines offer better efficiency and robustness than spark ignited (SI) engines [3]. These facts are crucial points in the cargo transportation sector, also called heavy-duty vehicles [4]. To increase the acceptance of CI engines, a further reduction of their exhaust emissions is necessary [5].

Combustion control is a potential alternative to avoid the production of NOx and particulate matter (PM) before treating them in the exhaust pipe. Several research centres are studying low-temperature combustion (LTC) concepts as a way to avoid the formation of these emissions [6][7][8].In this sense, it was found that a proper air-fuel mixture as well as the in-cylinder temperature stratification avoids the formation of these emissions. Additionally, an appropriate combustion control in the LTC concepts allows to improve the thermal efficiency compared to the conventional diesel combustion, even with a lower engine compression ratio [9]. Within the LTC concepts, there are several variants such as Homogeneous Charge Compression Ignition (HCCI) [10], Partially Premixed Combustion (PPC) [11], premixed charge compression ignition (PCCI) [12], Reactivity Controlled Compression Ignition (RCCI) [13][14] and Gasoline Compression Ignition (GCI) [15][16]. The main differences between these combustion strategies are related to the fuel composition, number of different fuels used and injection timing. The main limitation of all these strategies is the combustion control, since it mainly relies on the in-cylinder thermodynamic conditions due to the early injection timings promoted, and the high pressure rise rates found in the combustion chamber at relatively high loads. García et al. [17] proposed an intermediate solution where the ICE is calibrated to use RCCI at low and medium load, while a more diffusive combustion is implemented at high load. With this calibration approach, the NOx and soot emissions levels increase as compared to the single RCCI approach [18][19]. Therefore, depending on the operative conditions, as the driving cycle characteristics or the vehicle total weight, it could be not possible to achieve the EU VI emissions levels at engine-out conditions, which is the objective of this concept to reduce the aftertreatment costs. Other potential solution to avoid the ICE operation in the inefficient or restricted engine map zones with LTC is the use of an electric machine (EM) in the powertrain. Garcia et al. [20] proposed a de-rated RCCI engine in a parallel hybrid powertrain for medium-duty applications. The results show 15% of CO_2 reduction with respect to the commercial non-hybrid diesel truck with 90% of NOx and soot reduction. However, the study was limited to a single hybrid architecture. Other potential solutions such as: series hybrid successfully applied by IVECO in public buses [21][22] or power split in Toyota passenger vehicles [23] have not been tested.

Depending on the location of the electric machine, different hybrid vehicle configurations can be differentiated. The parallel architecture is widely used since it only uses an electric machine between the ICE and the transmission. It maintains several components of conventional vehicles with great advantages in terms of fuel

consumption [24]. The series architecture, also called range extender, is the simplest form of HEV architecture [25]. It decouples the combustion engine from the wheels making a separate ICE-generator system and on the other hand the traction motor connected to the differential that moves the wheels. Compared to other architectures, its operation and optimization is simple as well as it reduces transients in the ICE, making it possible to reduce its complexity. The power to operate in pure electric mode in general is greater than a parallel hybrid and the driving range is greater than an electric vehicle [26]. Other successful hybrid architecture implemented in passenger cars is the power split [27]. It has been globally recognized as an efficient and feasible architecture for developing hybrid electric vehicles. The power split architecture is classified into three types: 1) input-split, 2) output-split and 3) compound-split, depending on the arrangement between the ICE and the electric motors (generator and traction motor). In passenger cars, the Toyota Hybrid System [28] is the most widely used and can be classified as input-split. Its achievements in fuel economy and drivability have been highly praised. The Energy Management System (EMS) calibration will depend on the propulsion system, the type of vehicle and the operating conditions to which it will be subjected [29]. Prototyping and testing of each design combination is cumbersome, expensive, and time-consuming. Therefore, modelling and simulation are indispensable for the concept evaluation, prototyping and analysis of HEVs [30]. The main advantage of hybrid technology is the possibility of increasing the operational efficiency of the powertrain and regenerating the braking energy using an on-board energy storage system [31]. However, the benefits of the powertrains mentioned above are not widely discussed in vehicles such as trucks.

Therefore, the aim of this work is to study the potential of different hybrid architectures in a medium-duty truck with an internal combustion engine operating under RCCI combustion mode. Full hybrid operation is analysed under several driving cycles and vehicle payloads. In addition, a well-to-wheel (WTW) analysis is included to compare the potential of using an electrified fuel (or e-fuel) as low reactivity fuel in the RCCI combustion concept. These aspects are evaluated by means of a 0D-Vehicle model fed with experimental tests in an 8L six-cylinder compression ignition engine. To the knowledge of the authors, no work studying the potential of a hybrid propulsion system with advanced combustion in driving cycles for trucks has been done up to the moment. By contrast, all the studies found in the literature are focused on conventional combustion concepts where the aftertreatment system is complex and expensive. Additionally, in cargo vehicles the results are restricted to evaluations in homologation cycles and not in real cycles as those presented in the following work.

2. Methodology

The 0-D vehicle model of a Volvo truck platform with 18 ton of maximum payload was developed in the GT-Suite software. Table 1 shows the main characteristics of the vehicle under study. This segment of trucks is representative of the European medium-duty sector for urban-rural trajectories. In terms of power unit, the Volvo FL truck is equipped with an 8L six-cylinder diesel engine with a maximum power of 280 hp. The OEM truck is equipped also with a complex aftertreatment system (ATS) composed by: 1) Oxidation Catalyst (OC), 2) Particle filter (PF) and 3) Selective Catalytic Reduction with Urea (SCR-Urea) in order to achieve the EU VI normative. To reduce the vehicle cost and

improve the fuel consumption (CO_2 tailpipe emissions), the target of the present study is to remove the PF and SCR-Urea while improving the truck efficiency in transient conditions (driving cycles).

Table 1. Main vehicle specifications for 0-D model trucks

Base vehicle Mass [kg]	5240
Max Payload [kg]	12760
Vehicle Drag Coefficient [-]	0.65
Frontal Area [m^2]	5.52
Rolling friction [-]	0.0155
Tires Size [mm/%/inch]	295/80/22.5
Gear Box type [-]	6 gears manual
Differential ratio [-]	5.29
ICE rated power [hp]	280@2100rpm
ICE rated Torque [Nm]	1050

The main modifications on the base ICE include a new piston design for achieving a compression ratio (CR) of 12.8:1 instead of 17.5:1 (stock CDC engine), six port fuel injectors (PFI) to inject gasoline, and a low-pressure exhaust gas recirculation (LP-EGR) line. The other systems as the high-pressure exhaust gas recirculation (HP-EGR), the turbocompounding with a variable geometry turbine (VGT) and the direct injection diesel system are maintained from the stock engine. The engine is evaluated through stationary tests in 54 operative conditions in the range of 950 rpm to 2200 rpm and 10% to 100% of engine load. The calibration is performed with the objective of achieving EU VI NOx (<0.40 g/kWh) and EU VI soot (<10 mg/kWh) at engine-out conditions, and similar or better fuel consumption than CDC in all the engine map. The parameters to optimize are the injection timing of the high reactivity fuel (Diesel), the gasoline fraction (GF), EGR rate (both low pressure and high pressure) and VGT position for the abovementioned target. A detailed explanation of the calibration strategy can be found in a previous work of the research group [20]. The RCCI engine power was de-rated to 210 hp to reach the engine-out NOx and soot emissions targets imposed during the calibration. Then, the additional power needed to reach the OEM value (282 hp) will be supplied by the electrical machines. It is important to note that the results in this work are expressed in engine-out values. A summary of the ICE versions used in this work is depicted in Table 2.

Table 2. Main engine specifications for CDC and RCCI combustion

Parameter	CDC ICE	RCCI ICE
Type	4 stoke, 4 valves	4 stoke, 4 valves
Nº Cylinders	6	6
Displaced Volume [cm3]	7700	7700
Stroke [mm]	135	135
Bore [mm]	110	110
Injection type	DI diesel	DI diesel -PFI gasoline
Compression ratio [-]	17.5:1	12.8:1
High pressure EGR	Yes	Yes
Low pressure EGR	No	Yes
Turbo Configuration	VGT	VGT
Rated Power [hp]	282@2000rpm	210@2200rpm
Rated Torque [Nm]	1151@1500rpm	858@1500rpm

To promote RCCI operation, the high reactivity fuel (HRF) used is a commercial diesel injected by means of the original direct injectors and the low reactivity fuel (LRF) is a commercial gasoline injected by the PFIs. The ratio of the gasoline mass over the total mass is referred to as gasoline fraction (GF).

Figure 1 shows the calibration maps of fuel consumption, tailpipe CO_2 emissions, EGR rate, GF and engine-out NOx and soot emissions at brake conditions. The de-rating of the engine is seen in the difference between the achieved calibration 210 hp (black line) and the OEM diesel calibration of 280 hp (red line). These maps are used as inputs in the 0D vehicle model for the hybrid versions [32]. The target of the design of the powertrain is at least to achieve the same power output than the OEM case.

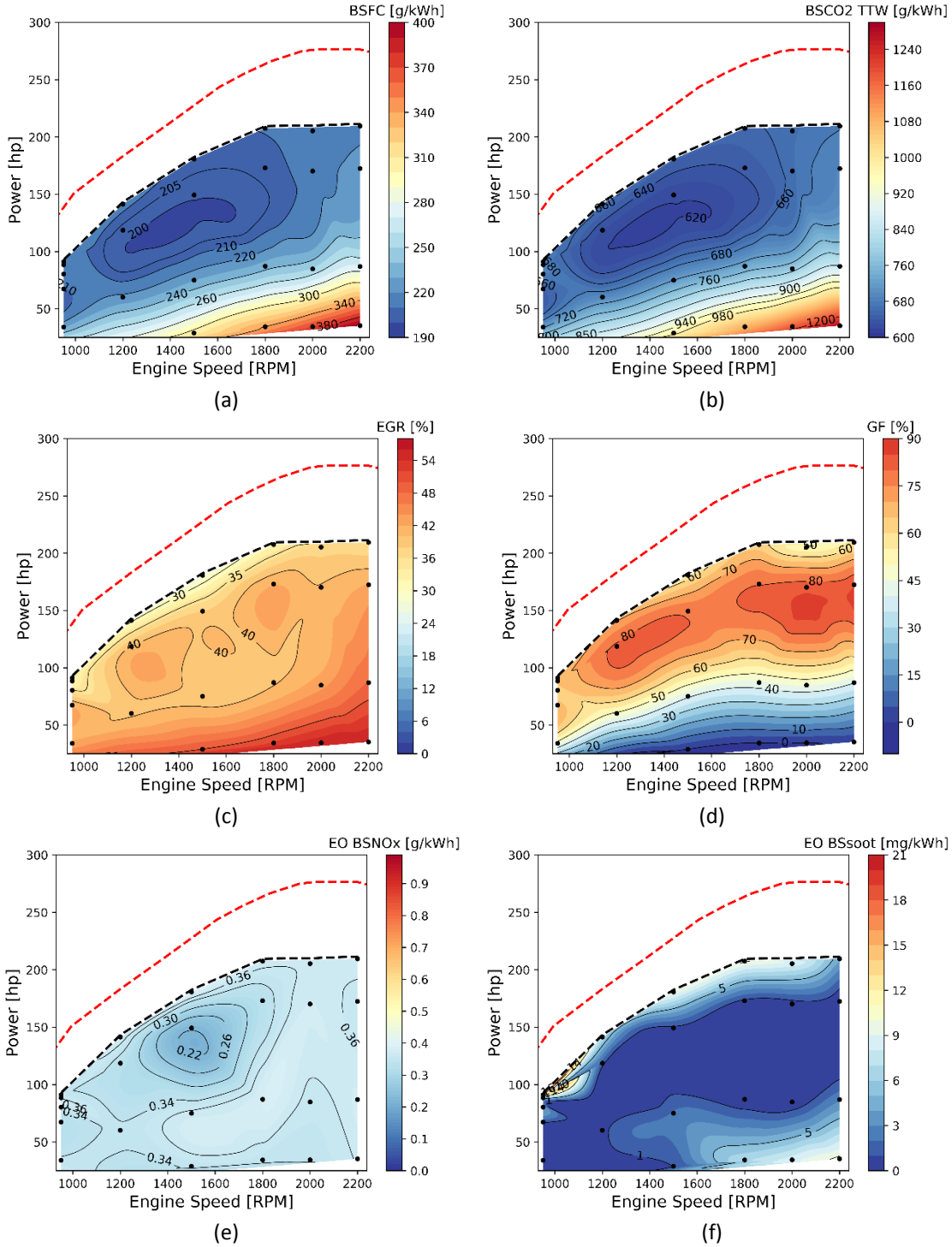

Figure 1. Engine calibration maps for the RCCI 8 litres multi-cylinder Volvo ICE. Brake specific fuel consumption (a), Brake specific CO_2 tailpipe emissions (b), Exhaust gas recirculation rate (c), Gasoline fraction (d), Engine out brake specific NOx emissions (e) and Engine out brake specific soot emissions. The dashed line marks the maximum power of the originally CDC calibration (red colour) and RCCI new calibration (black colour).

The resistive forces to model the truck platforms are obtained with road measurements of the commercial non-hybrid truck and depicted in Table 1. To assemble the hybrid powertrains, the electric components (battery pack, electric machines, inverters, controllers, among others) were inserted in the driveline. The proposed P2 RCCI hybrid truck is shown in Figure 2a. A single electric machine (operate as motor or

as generator) is coupled to the ICE and the manual six gear OEM transmission by an additional clutch. Figure 2 also shows that an additional fuel tank for the gasoline is added in the vehicle scheme. In the P2, to achieve the same maximum power of the non-hybrid version (280 hp), an EM with 70 hp is added to compensate the 210 hp of the RCCI ICE. As mentioned previously, the main advantage of the P2 architecture is the relative small number of changes needed compared to the original powertrain [33].

Figure 2b shows the series architecture with the ICE-generator in the frontal part of the truck and the traction motor in the back coupled to the wheels by the axle and the final drive. The battery package and the extra fuel tank are in the same location than in the P2. The generator has the same maximum power than the RCCI ICE (210 hp) and the traction motor equal to the non-hybrid ICE version (280 hp). Due to the separation of the ICE to the wheels, it requires electric machines with higher power than the P2. Due to the absence of transmission, the final drive is optimized in the parametric analysis.

Figure 2c shows the power split architecture. It is an intermediate case between the P2 and series. It connects the ICE to the wheels through a power split device. This special transmission has three engagements. One for the ICE, the second for a generator and the third for the traction motor. In the Figure 2c, the generator is located inside the PSD. Therefore, it is called e-PSD. The configuration used is input-split, similar to the well-known solution used in the Toyota Prius [34]. The main purpose of the e-PSD is to control the ICE to operate in the best operation zone (line of minimum BSFC) but with direct connection to the wheels. This could have benefits in terms of reduction of the electric losses at high speed or high payloads. Like the series architecture, the final drive is optimized by means of a design of experiments.

In all the cases, a full hybrid electrified version is selected with the aim to target 2025 limits (15% CO_2 reduction). A micro-hybrid version will imply a very low CO_2 reduction while a plug-in hybrid version will require many modifications with respect to the OEM truck.

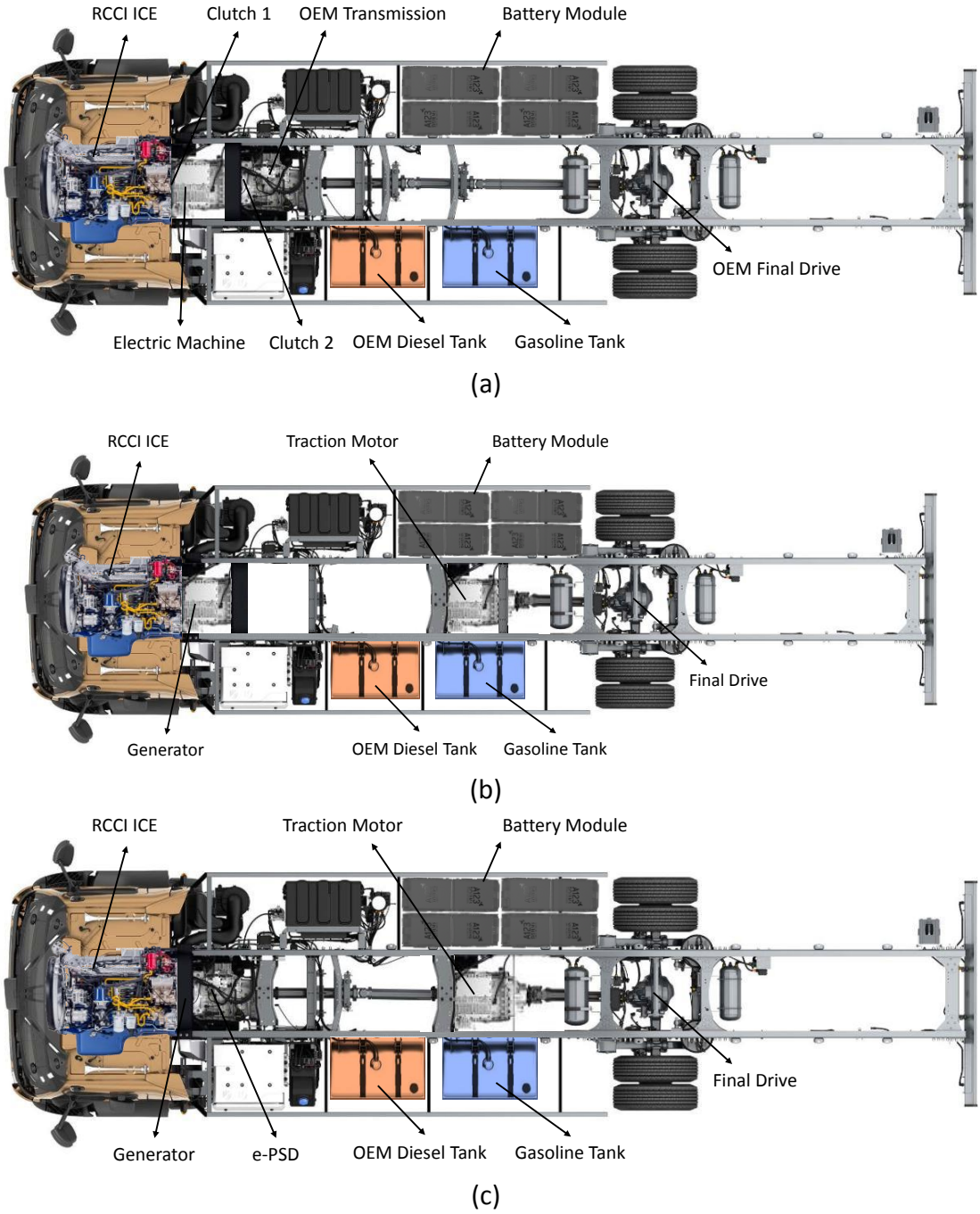

Figure 2. Hybrid architectures for the RCCI truck concept. P2 (a), Series (b) and Power Split (c).

For simplicity and robustness, a rule-based control (RBC) type EMS has been used [5]. In the P2 architecture, four modes are differentiated. 1) Pure electric: the EM in traction mode propels the vehicle with the ICE off. 2) Battery charging: the ICE is turned on to power the vehicle and charge the battery (EM works as a generator) at the same time. 3) Boost mode: ICE and EM (traction mode) deliver power at the same time to propel the vehicle. The maximum powertrain brake torque is achieved in this mode. 4) Regenerative braking: the ICE is turned off and the EM operates as a generator recovering energy from the deceleration. It is important to note that the speed of the ICE depends on the speed of the wheel by a multiplication in the final drive and the transmission. A detailed explanation on the RBC strategy for P2 can be found in [35].

In the series architecture the ICE is decoupled from the wheels, so it has differences in the operative conditions compared to the P2. However, similarities as the pure electric mode and regenerative braking are found. As the TM is larger than in the case of the P2, higher electric driving range and brake energy recovery can be done. The main difference is that it does not exist a mode where the ICE propels the vehicle. Always, the ICE is turned-on to generate energy by means of an electric generator. A three-level strategy is used depending on the battery state of charge (SOC). The arrangement was done following equally separated SOC levels. The lower the SOC level, the higher power generated by the ICE. In the third level, the 210 hp is delivered by the RCCI ICE. The other two operative conditions are selected in the optimization section by a search in the minimum BSFC line.

The RBC for the power split was created as a mix of both cases. The e-PSD allows to control the ICE speed by means of a generator motor. A signal of the desired speed in the ICE is sent to the generator, and a PID controls the torque output of this EM. The desired ICE speed is obtained by means of other PID that calculates the target power for the battery charging. This power is translated in an operative condition in the minimum BSFC line. In addition, a top speed for pure electric mode and hybrid mode is included. Therefore, the vehicle can be propelled by the TM in pure electric driving, regenerate energy in the braking phases and be propelled directly with the ICE at a desired operative condition.

The control parameters (RBC rules) and battery size were calibrated by means of a genetic algorithm. The last aforementioned component is crucial because it has a strong influence on the final vehicle cost, vehicle weight and electric driving range, among others. The battery is modelled by means of a validated equivalent electrical circuit model with cylindrical cells of Li-FePO4 produced by A123 Systems [36]. Lastly, the electric machine is modelled based on the JMAG motor design tool [37]. The targets of maximum power and rotational speed are set depending on the hybrid architecture. The electric machine is not optimized because it is selected to obtain the same maximum brake power in the hybrid than in the non-hybrid version. The additional weight was also obtained from JMAG and included in the vehicle model.

Table 3 shows a summary of the range of values for the control system and components optimization. It is important to remark that the gear shift strategy for P2 is the ICE speed at which the gear change is made in the OEM six gear transmission. The maximum pure electric mode speed (P2 and power split) is the maximum vehicle speed with the ICE turned-off. Lastly, two control parameters are used to maintain the battery state of charge (SOC). One is the minimum SOC at which the battery needs to start charging and the other parameter is used to control a PID to obtain the desired power to charge the battery. If the SOC achieves the maximum value, then the maximum electric power is delivered. Between this value and the initial SOC, a proportional PID is used to control the electric charge. All the parameters were studied in a wide range considering commercial components availability (battery, final drive ratio) and the

possible control space (ICE rotational speed, battery SOC variation, vehicle speed and split ratio).

Table 3. Optimum hybrid powertrain set up.

Parameter	Type of parameters	Architecture	Range Tested
Battery Size	Hardware	P2	8-80 kWh
		Series	
		Power Split	
Final Drive ratio		Series	2:1 – 12:1
		Power Split	
Gear shift Strategy	Control transmission	P2	1300 – 2200 rpm
Maximum Pure Electric mode speed	Control electric machine	P2	5 – 120 km/h
		Power Split	
Split mode between ICE and EM		P2	0 – 100 %
ICE operative condition		Series	60-210 hp
SOC start charge	Control battery pack	P2	0.45 – 0.58
		Series	
		Power Split	
SOC maximum to charge		P2	
		Series	

The target for the genetic algorithm (Genetic Algorithm NSGA-III [38]) is to minimize fuel consumption while reaching the same battery SOC at the end of the driving cycle than the initial SOC. An additional constrain is added to fulfil the EU VI NOx and soot target at the end of the cycle without ATS. It is important to note that this is possible thanks to the RCCI ultra-low emissions values. The space over which the factors are varied is called the design space and it is shown in Table 3. All the cases out of the constraint conditions are eliminated. The five key inputs required for the NSGA-III are the population size (P_s=40), crossover rate (C_r=1), crossover rate distribution index (C_{rdi}=15), mutation rate distribution index (M_{ri}=20) and number of generations to run (N_g=20). The optimizer will stop after completing all the designs according to the number of generations. This optimizer is applied in a transient condition previously set. A sensitivity analysis is also included to analyze the effect of the control parameters in the final fuel consumption and battery SOC. The relative sensitivity values are calculated by dividing the absolute value of each regression coefficient by the sum of the absolute values of all the regression coefficients. The linear regression equation is shown in equation 1:

$$y = a_0 + a_1 x_1 + a_2 x_2 + \cdots + a_n x_n \quad (1a)$$

$$S_i = \frac{|a_n|}{\sum |a_i|} \quad (1b)$$

where x_1 represents the standardized factors, a_i represents the standardized regression coefficients, y represents the standardized response and S_i represents the sensitivity values.

The vehicle is tested in four transient conditions (see Figure 3) representative of the homologation conditions (WHVC) and real driving routes. In addition, the payload is set at 0%, 50% and 100%. Therefore, 12 different conditions are used to evaluate the non-hybrid and hybrid powertrains. For the powertrain optimization, the WHVC at 50% payload is used, as it is representative of the European homologation for heavy-duty trucks.

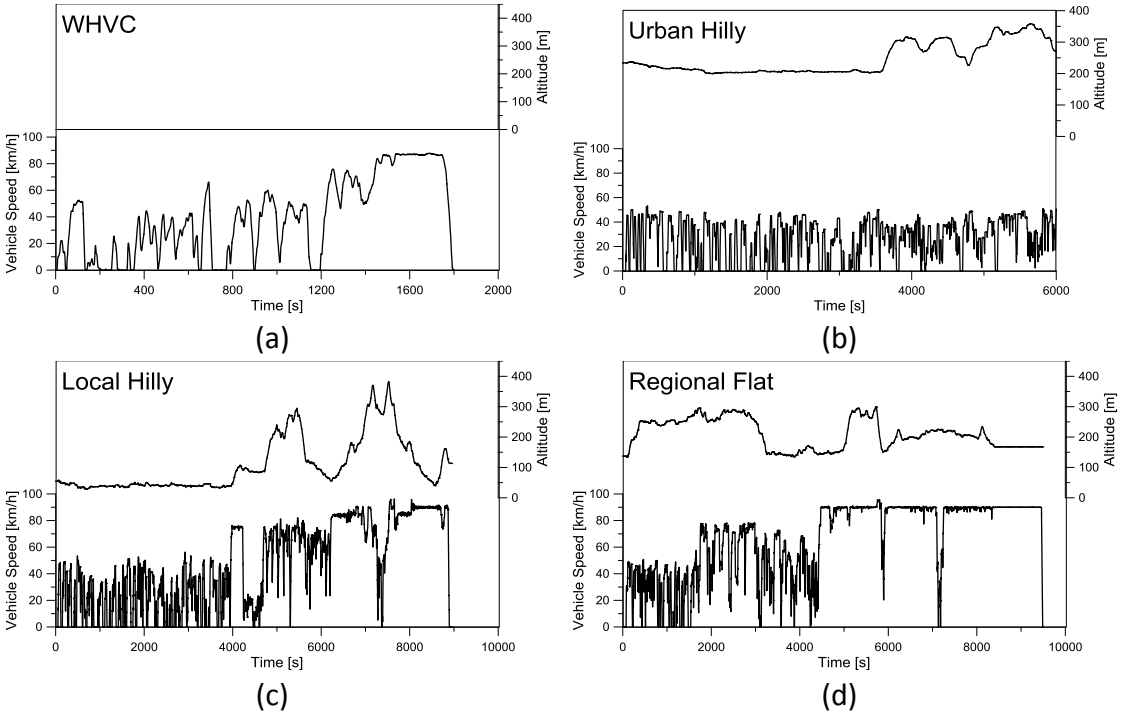

Figure 3. Driving Cycles, speed and altitude against time, for the 0D vehicle model in WHVC and (a) and real routes called Urban Hilly (b), Local Hilly (c) and Regional Flat (d).

A well-to-wheel analysis is considered in this work to evaluate the potential of using e-fuels in a hybrid RCCI powertrain. Figure 4 shows a scheme of the different e-fuels that can be obtained using renewable electric energy, carbon capture and clean hydrogen production. Fuels as OMEx, synthetic gasoline, synthetic kerosene, synthetic diesel and synthetic lubricants can be obtained. The difference between blue and green fuel is the H_2 production process, with the blue one coming from steam-methane reforming and the green one coming from water electrolysis with renewable energy [39]. For this work, due to the already existing calibration of the RCCI ICE with diesel-gasoline, and the proved similarities among the synthetic gasoline and the commercial one in terms of final performance [40], synthetic green gasoline is selected. By means of a WTW analysis in GaBi commercial software, a maximum of 3.0 gCO_2/MJ of synthetic gasoline produced from the less carbon intensive methanol pathway, with either green or blue hydrogen, is obtained in a WTW CO_2 basis. This leads to a 97% of CO_2 reduction with respect to commercial gasoline. The values for diesel and gasoline production were also obtained with GaBi, with a WTT value of 18.6 gCO_2/MJ for diesel and 17.2 gCO_2/MJ for gasoline. The well-to-tank value for synthetic gasoline is -70 gCO_2/MJ of fuel

produced thanks to the carbon capture and the low carbon energy production considered in the process.

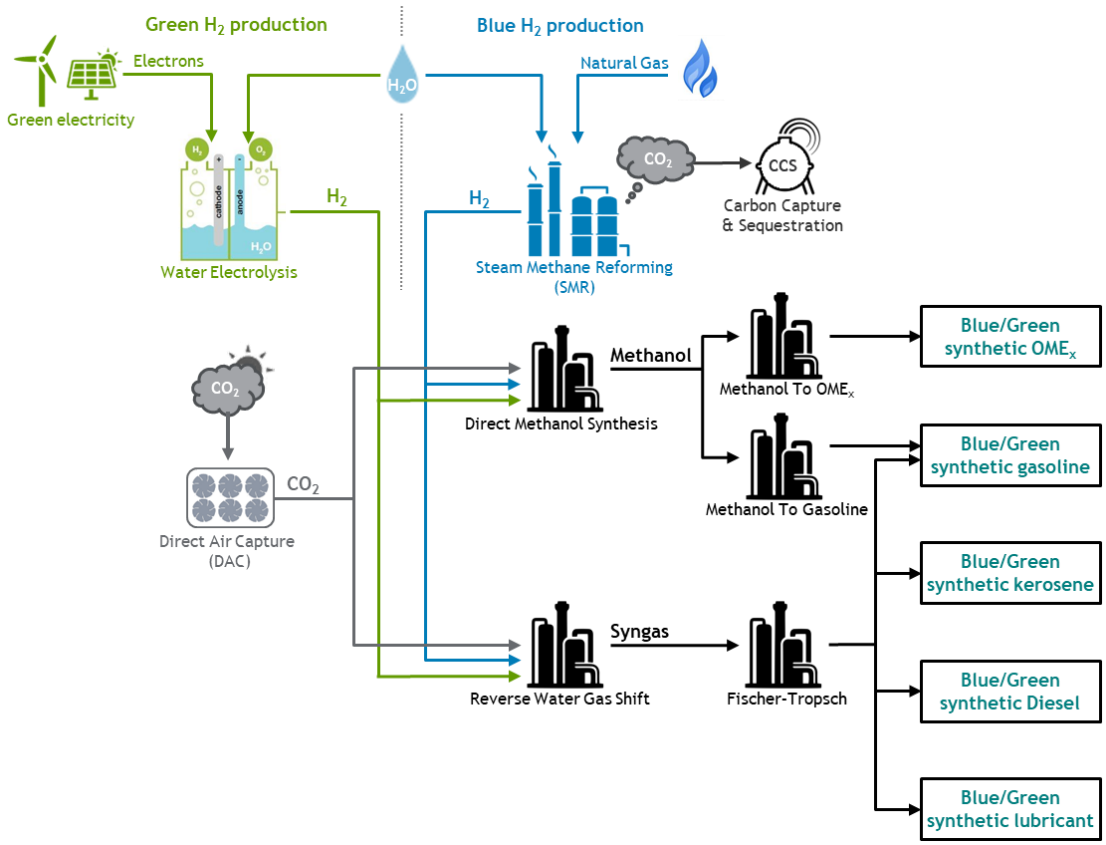

Figure 4. Fuel production pathway for synthetic fuels from carbon capture, low carbon electricity and low carbon hydrogen.

3. Results and Discussion

The results are divided into three main subsections. First, the performance of the RCCI hybrid powertrain using e-fuels are presented against the conventional powertrain for several vehicle speeds and elevation grades. Later, the optimization results about the impact of the battery size on the CO_2 reduction are showed. Lastly, the global results with the optimum values are presented.

3.1. Performance Results

The vehicle performance is a crucial aspect of the truck. With the introduction of new powertrains, the OEMs are pursuing the fuel consumption reduction without losing vehicle's drivability. From the perspective of the users, they desire to not suffer big changes in terms of vehicle operation and refuelling time. Therefore, the powertrain design target is to achieve similar wheel force, simplicity in user operation and energy charging time. The last point is guaranteed by selecting a full hybrid instead of plug-in hybrid powertrain. Moreover, it has been found that the use of two tanks of liquid fuel increases the refuelling time when changing the fuel hose by less than 5 minutes.

To study the powertrain performance, several vehicle speeds and road grades were simulated. This study was done considering the vehicle with 100% payload (worst

condition) for the four powertrain cases. The conventional architecture is taken as baseline for all the hybrid cases as is already tested in commercial applications. The objective of this section is to understand if the electric machine size selection based in achieving the same power output than the OEM truck is appropriate.

Figure 5 shows the P2 hybrid powertrain against the CDC non-hybrid in two different modes. In pure electric mode (only the 70 hp EM is delivering power) the vehicle has constant force in the wheels up to a set speed, depending on the gear in the transmission, and then a constant decay in the power curve is seen. This behaviour is totally different of that from the conventional powertrain, which shows an increase of the wheel force up to a set speed (corresponding to the maximum ICE torque), and then decays down to the limit speed of the ICE. This behaviour is due to the different characteristics of the EM versus the ICE. In addition, wheel force in pure EV mode is lower than the conventional powertrain due to the selection of a 70 hp EM (to reach a total 280 hp when combined with the 210 hp ICE). However, the truck can be driven in road grades higher than 7% with vehicle speeds up to 10 km/h. The maximum vehicle speed in pure EV mode is 70 km/h in a flat road. It is important to note that these values are calculated for the most demanding condition, 100% payload (18 ton). The boost mode in a P2 architecture is the sum of the maximum power of the ICE and the EM. Figure 5 shows that is possible to achieve higher wheel force in almost all the vehicle speeds. The curves intersect at the limit speed for each gear, which corresponds to 2200 rpm of the ICE, due to the condition imposed for the P2 that forces the power of the ICE+EM to be equal to the ICE power in the conventional vehicle. This depicts the best performance of the P2 when is working the boost mode. As it is a full hybrid, the energy needs to be recovered by charging the batteries with the EM in generator mode. Therefore, the boost mode can be used in limited periods of time. The next section shows the vehicle in real driving conditions to analyses this point in detail.

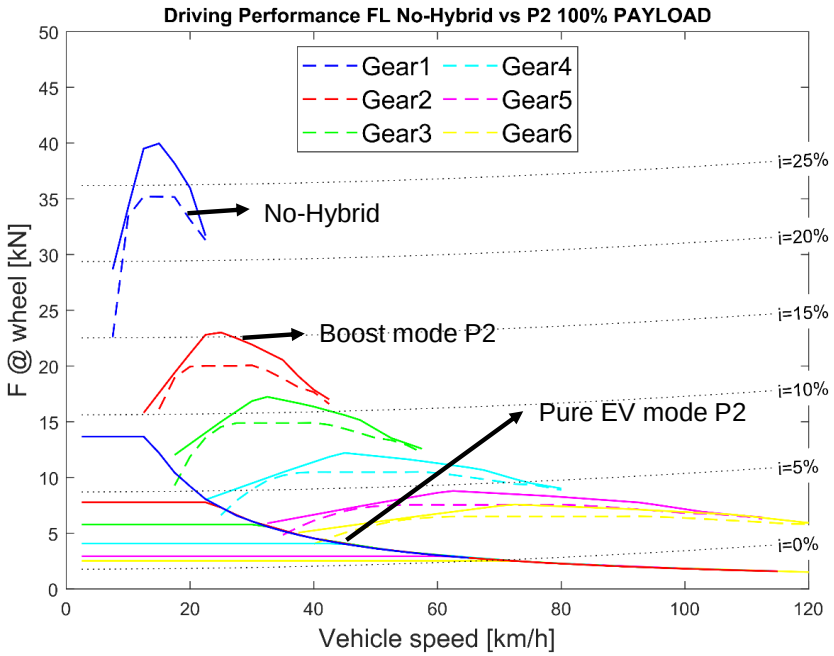

Figure 5. P2 performance graph with the two modes and compared against the non-hybrid configuration.

The series, or range extender, truck performance is tested in the same conditions than the P2, and the results are depicted in Figure 6. The two different modes are plotted against the conventional case. In pure electric mode, in which the ICE is turned-off and the TM is consuming energy only from the battery, the series truck has higher wheel force in all vehicle speeds except for the first gear. The pure EV curve intersects with the non-hybrid ones in the extreme vehicle speed for each gear due to the selection of the same power for the TM than the ICE in the non-hybrid configuration (280 hp). In addition, due to the absence of transmission in the series hybrid, the wheel force does not have jumps as in the non-hybrid version. The second mode for the series, range extender, takes place when the battery is depleted, and the power is delivered by the ICE-generator (210 hp) and passed to the TM. In this case, the wheel force is limited by the ICE-generator and depends on the vehicle speed. Then, the wheel force can be above (low vehicle speed) or below (high vehicle speed) than the non-hybrid case. In any case, the Figure 6 shows that it is possible to achieve the maximum vehicle speed in a flat road and up to 60 km/h with a grade of 5%.

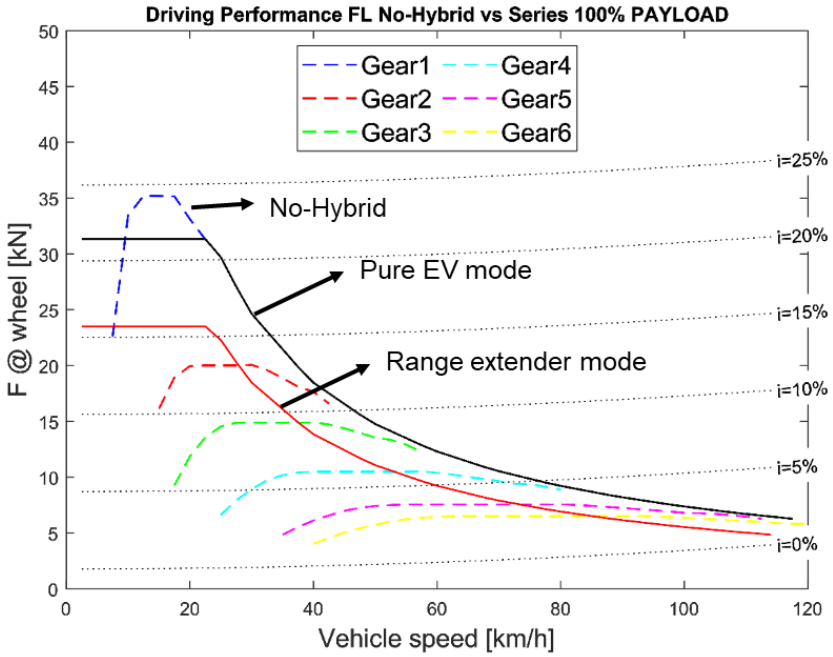

Figure 6. Series performance graph with the two modes and compared against the non-hybrid configuration.

The power split has a complex operation, and the maximum performance needs to be obtained after several iterations. As this solution is a combination of parallel and series, both behaviours are seen in this powertrain (Figure 7). The pure EV mode, where only the TM is propelling the vehicle, has the same trend than the series but with less wheel torque due to the lower EM power and lower differential ratio. However, the truck can achieve the maximum vehicle speed in a flat road and operating in roads with 15% of grade at vehicle speed less than 20 km/h. The boost mode depends on the

generator rotational speed. With a well calibrated controller, it is possible to achieve a similar curve to a pure EV. The wheel toque is almost above the non-hybrid powertrain for all the vehicle range.

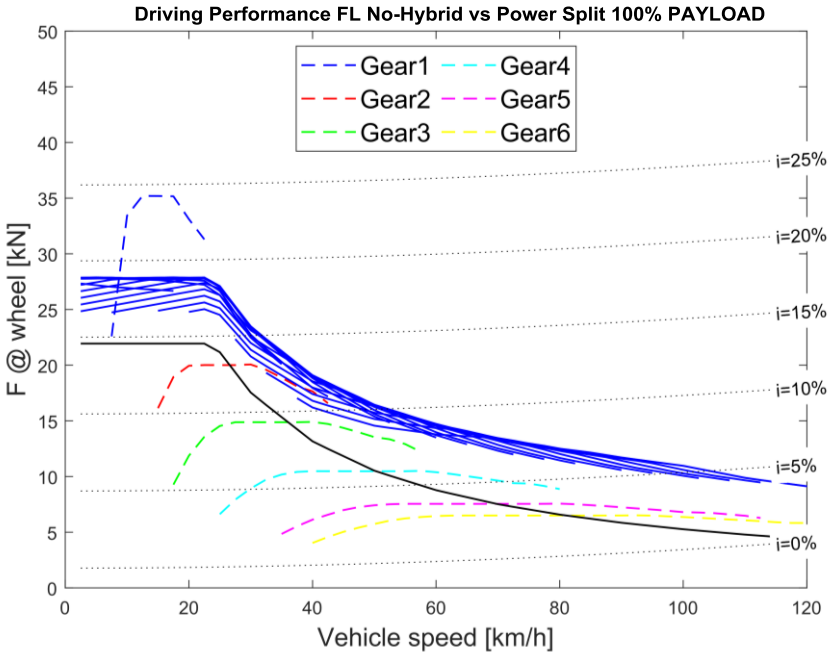

Figure 7. Power split performance graph with the two modes and compared against the non-hybrid configuration.

From the previous analysis, it can be said that the hybrid version has better performance than the non-hybrid case with the selected components. The de-rated RCCI ICE is well compensated by the electric machines to achieve higher wheel torque in almost all the conditions. However, some modes have a limitation in the time of use. Therefore, the battery size needs to be deeply studied in real driving cycles to understand the requirements and the benefits in terms of fuel consumption and emissions.

3.2. Optimization Results

The right selection of the battery size and the optimization of the energy management control in hybrid powertrains is crucial to obtain benefits in terms of fuel consumption and emissions. For this work, the target is to obtain the minimum CO_2 emissions (minimum fuel consumption) while meeting EU VI engine-out NOx and soot emissions under the WHVC at 50% payload (homologation conditions). The genetic algorithm allows to optimize the design parameters for the above-mentioned target. Figure 8 shows the fuel consumption with the evolution of the genetic algorithm generations for the three hybrid architectures. In the colour bar is added the battery SOC at the end of the cycle, which needs to arrive at least up to 60% ($SOC_{initial}$). The cross marks show the cases in which this constrain is not achieved. After the first 150 cases the genetic algorithm concentrates the generated cases in a narrow fuel consumption zone. The power split is the powertrain that depicts the largest dispersion. This is

possible to explain due to the difficulties to control the ICE operation zone by the generator and the several possible split between pure electric and different ICE operation. Moreover, the P2 architecture achieves the lowest fuel consumption followed by the series and closely by the power Split. The use of only one EM allows to reduce the electric losses and the braking phase does not require highest EM power for this operative case.

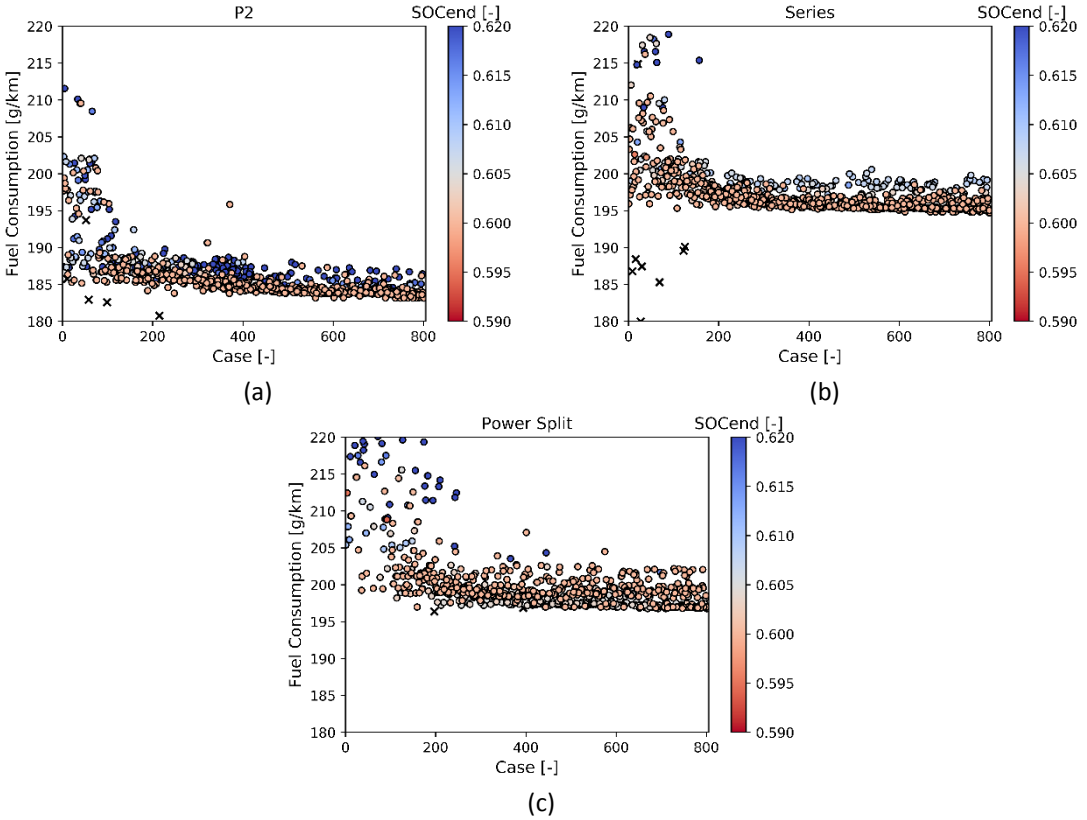

Figure 8. Fuel consumption in WHVC at 50% payload for the 800 cases generated in the GA and the final battery state of charge. Cross marks represent the cases that violet the constrains.

An important aspect is the effect of the calibration parameters in the fuel consumption and the final battery SOC. Figure 9 shows the sensitivity of the parameters in the abovementioned outputs. For the P2, the most sensitive parameter is the shift strategy. This parameter controls the engine speed and torque delivered by the ICE. The battery is an important aspect in the final SOC but does not have a large effect on the fuel consumption. This is a positive point because it allows to reduce the battery size and the powertrain cost. For the series powertrain, the actual SOC to start charge (SOC width) in each power level is the most influence parameter. In addition, the battery size has more influence than in the case of P2. Lastly, the power split has large dependence in the maximum EV mode speed for both fuel consumption and final SOC. The other parameters have similar weight in the sensitivity analysis.

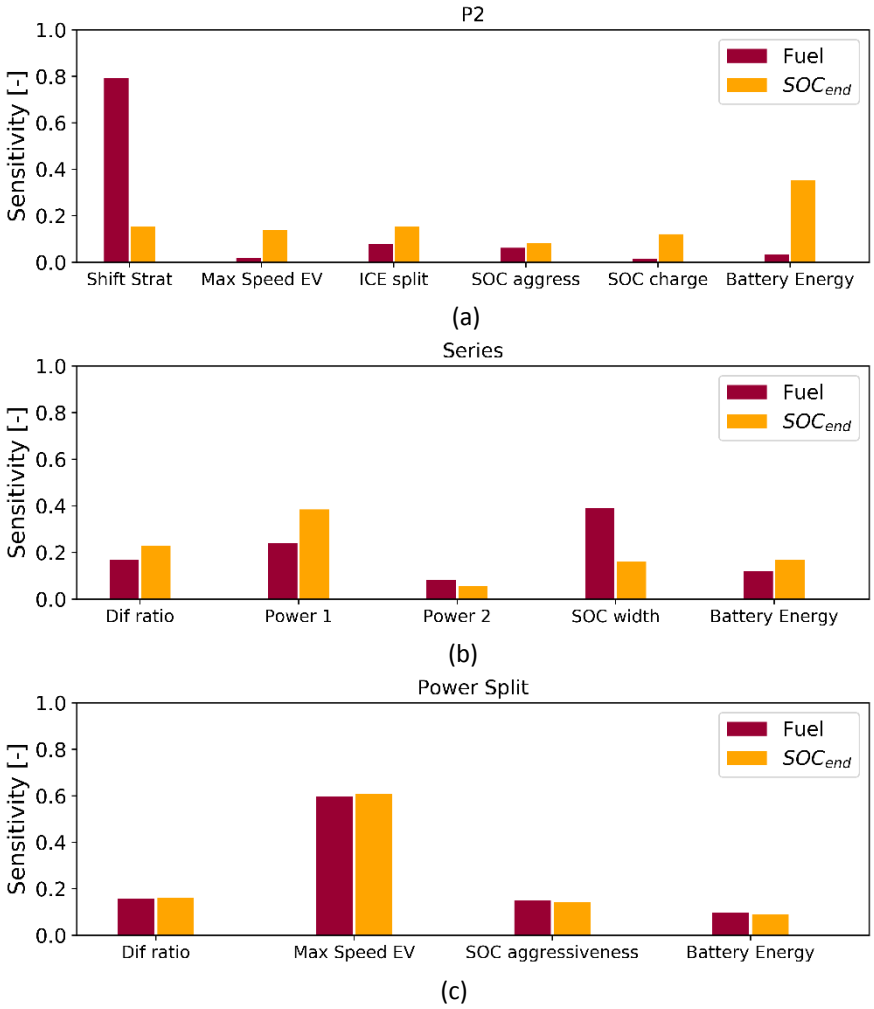

Figure 9. Genetic algorithm sensitivity for the design parameters in the WHVC at 50% payload for the P2 (a), Series (b) and Power Split (c) architectures.

Figure 10 shows the fuel consumption benefits with respect to the baseline (OEM non-hybrid CDC truck) as a function of the battery size and the most influencing parameters. For the P2, the battery size has lower effect with the optimum at 8 kWh (minimum of the range tested). The shift strategy is preferred to be close to 1300 rpm because is possible to shift the operative points to high engine loads. The series and power split preferred a higher battery capacity (around 40 kWh) to reduce the fuel consumption. In addition, a large battery width for the series allows to extend the use of the first power level. The optimum selected configuration for each powertrain is shown in Table 4.

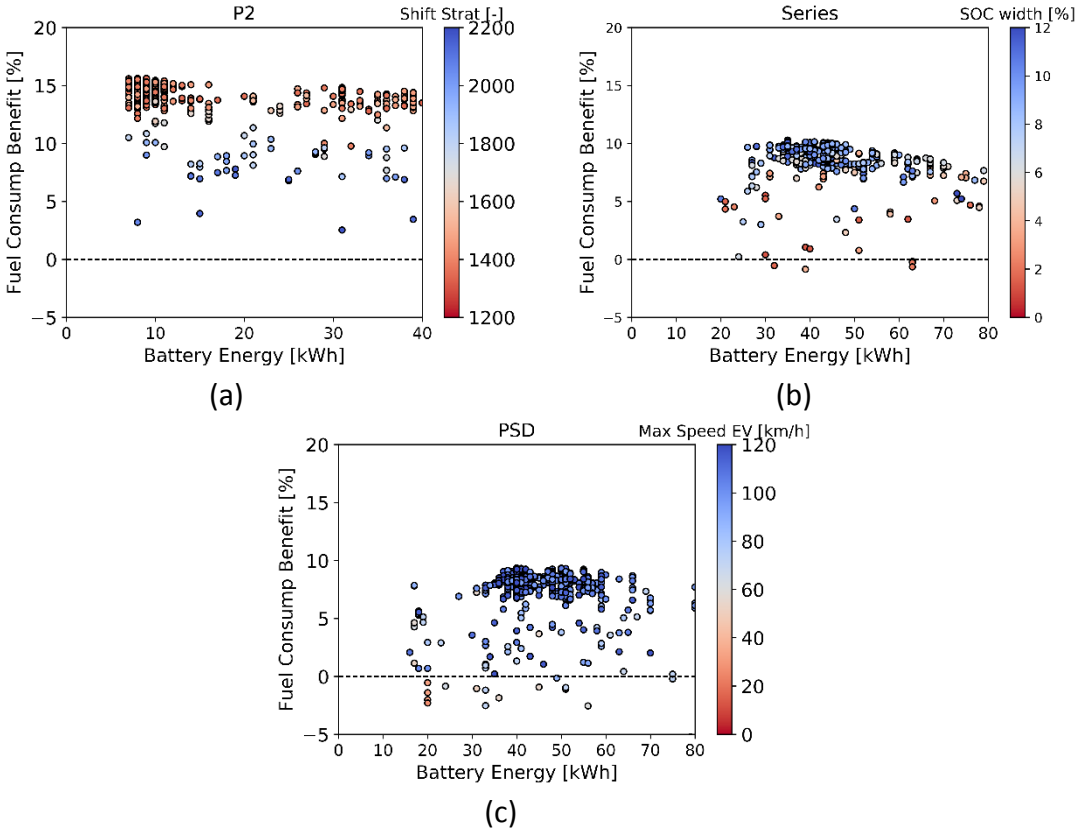

Figure 10. Fuel consumption against the battery energy in WHVC at 50% payload for the 800 cases generated in the GA. The colour bar shows the main parameter obtained from the sensitivity analysis: P2-Shift strategy (a), Series-SOC width (b) and Power Split-Maximum Speed in pure electric mode (c).

Table 4. Optimum hybrid powertrain set up.

Parameter	Type of parameters	Architecture	Range Tested
Battery Size	Hardware	P2	8 kWh
		Series	42 kWh
		Power Split	47 kWh
Final Drive ratio		Series	8.2:1
		Power Split	8.6:1
Gear shift Strategy	Control transmission	P2	1360 rpm
Maximum Pure Electric mode speed	Control electric machine	P2	9.4 km/h
		Power Split	93 km/h
Split mode between ICE and EM		P2	0 %
ICE operative condition		Series	98 kW / 156kW
SOC start charge	Control battery pack	P2	0.491
		Series	0.565 / 0.529
		Power Split	0.549
SOC maximum to charge		P2	0.505
		Series	0.494

From the previous analysis, it is inferred that all the hybrid powertrains can help the OEM to reduce fuel consumption and CO_2 emissions of their vehicle fleets. Moreover, the P2 seems to be the most advantageous architecture compared to the series and power split.

3.3. Global Results

The optimum cases are analyzed in terms of powertrain behaviour and final value for the WHVC 50% load cycle. Figure 11 shows the instantaneous power against the engine speed values in the engine calibration BSFC map. It is important to note that, for confidentiality reasons, the BSFC CDC map was not represented for the non-hybrid case. On the contrary, the DMDF map was presented. As the main purpose of this graph is to see the operation of the different architectures, this figure still meets the abovementioned objective. Each point represents one second of operation in the WHVC with 100% of payload. The non-hybrid DMDF and P2 have operative points in several engine speed and almost all the loads. The main difference between these two architectures is that the P2 reduces the operative conditions at low loads. In this sense, the optimization of the energy management system, by controlling the gear shift strategy and the electric machine operation, allows to concentrate the operative conditions in a range of intermediate engine speed (950 rpm to 1500 rpm) and ICE high load zone, where its operation is more efficient. In addition, it is possible to see that the engine de-rating from 280 hp to 210 hp does not represent any limitation at full payload.

On the other hand, the series and power split show a totally different operation behaviour. The series is only operated in two operative conditions, 1200 rpm and 125 hp and 1900 rpm and 170 hp, both in the optimum fuel consumption zones (below 210 g/kWh). The level 3 of charge, which corresponds to 210 hp, is not used due to the high energy content of the battery selected. However, for more demanding cases as Regional Flat (Figure 3d) with long routes it would be used. The power split has similar behaviour but uses a line of operative conditions that are under the best BSFC line. For the power split, the transient variation is larger than the series but more controlled than in the P2. This behaviour is thanks to the dedicated generator that controls the ICE by the decoupling from the wheels speed. In advanced combustion concepts, this is a benefit because help to solve issues as combustion control, high EGR rate changes among other parameters.

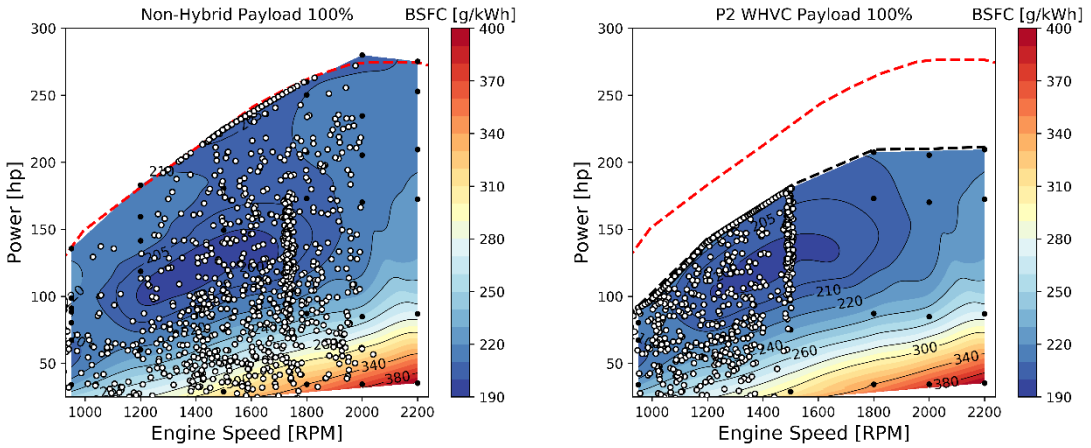

(a) (b)

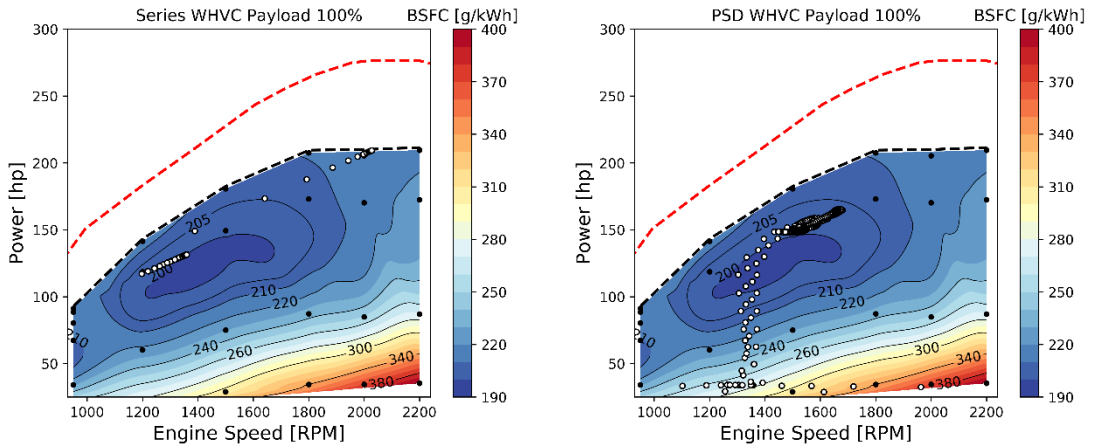

Figure 11. ICE operative conditions for WHVC and 100% payload in the four powertrains: non-hybrid DMDF (a), P2 (b), Series (c) and Power Split (d).

The optimum powertrain selection is studied in other 3 different driving cycles (see Figure 3) at 0%, 50% and 100% of payload. The simulation guarantee that the final vehicle SOC is at least equal than the initial SOC. In the case of not achieving the final SOC, one additional minute is maintained with the vehicle stopped for the ICE to re-charge the battery pack. Figure 12a shows the tank-to-wheel CO_2 emissions reduction with respect to the baseline case. In addition, the 2025 European Target (15% with respect to 2019) is marked in dashed line. All the hybrid powertrains show CO_2 reductions when the truck is unloaded. In addition, the urban case has also the highest benefits for all the load conditions. Comparing the powertrain architectures, the P2 has the largest benefits, only improved in the series and power split at low payload and large combined cycles (local and flat). The engine-out NOx and soot emissions showed in Figure 12b and Figure 12c highlight the benefits using RCCI combustion. For all the cases, the emissions achieved the EU VI legislation limits and around 90% improvement with respect to the baseline.

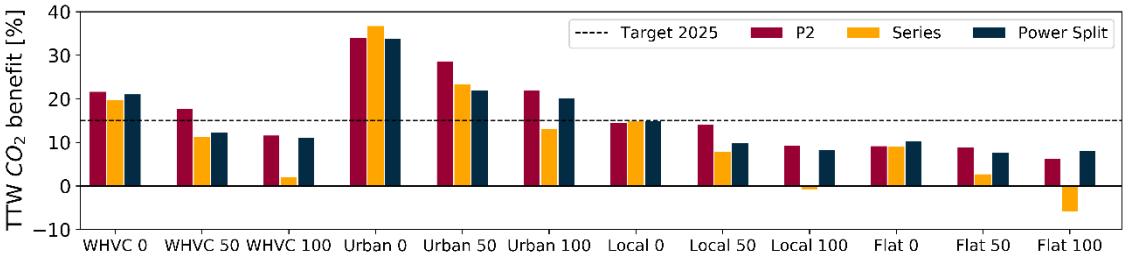

(a)

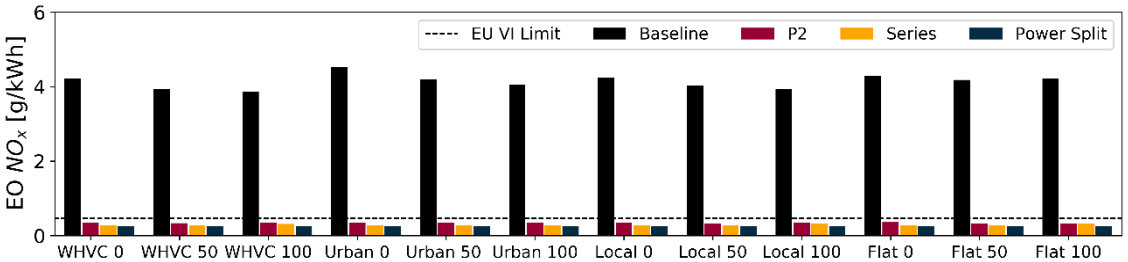

(b)

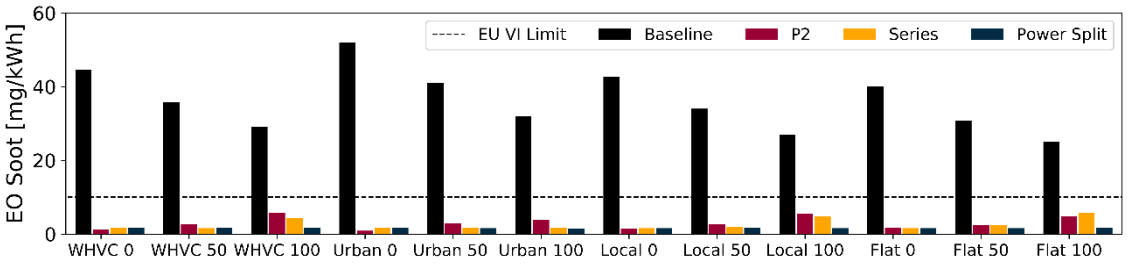

(c)

Figure 12. TTW CO_2 emissions benefits (a), engine out NOx emissions (b) and engine out soot emissions (c) for four driving cycles and three payload conditions.

Figure 13 includes an energy analysis to investigate the benefits in fuel consumption (TTW CO_2 emissions). Figure 13a depicts the ICE average brake thermal efficiency of the cycle. It possible to see that the highest ICE improvements are at low payload conditions where the non-hybrid operates in low efficient zones. In addition, due to the totally or partially uncoupling of the wheels, the series and power split achieve almost 42% BTE independently on the payload. Figure 13b shows the energy recovered during braking with respect to the tractive energy necessary to meet the speed during acceleration. The urban cycle is the only cycle that increases the recovery with the payload. The other cycles show the highest recovery at 0% payload in general. As highest the rural and highway phase, the energy recovery decrease with the payload as seen for the Flat with respect to the Local cycles (Figure 3). The P2 is the powertrain that has the lowest brake recovery due to electric machine limitations. However, Figure 13c shows that using one electric machine, as the case of P2, allows to reduce the electric losses compared to the series and power split, which require a traction motor and generator separately. Although the electric losses consider the battery losses, it is not seen a large variation between powertrains.

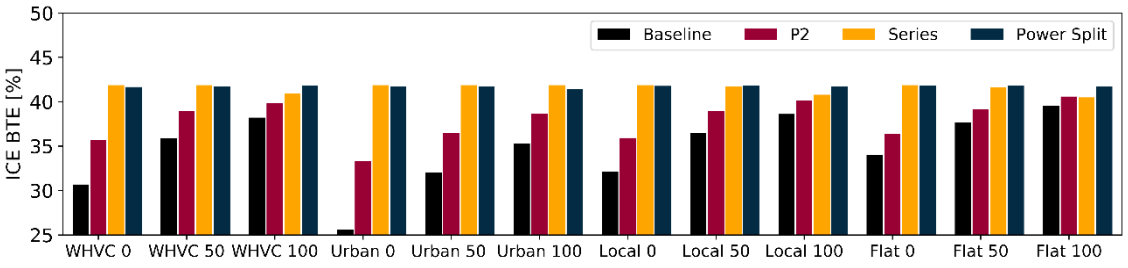

(a)

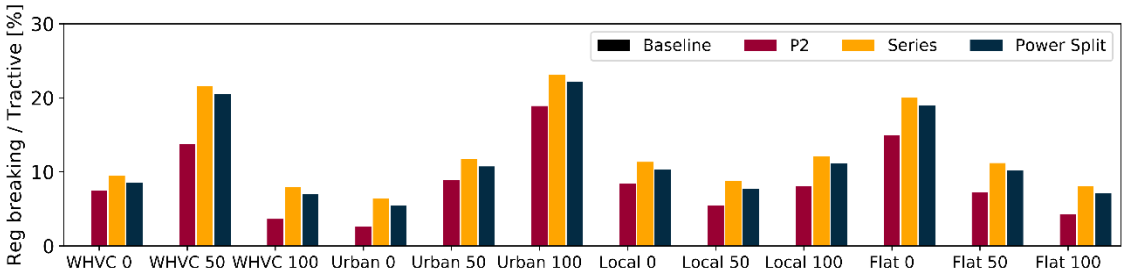

(b)

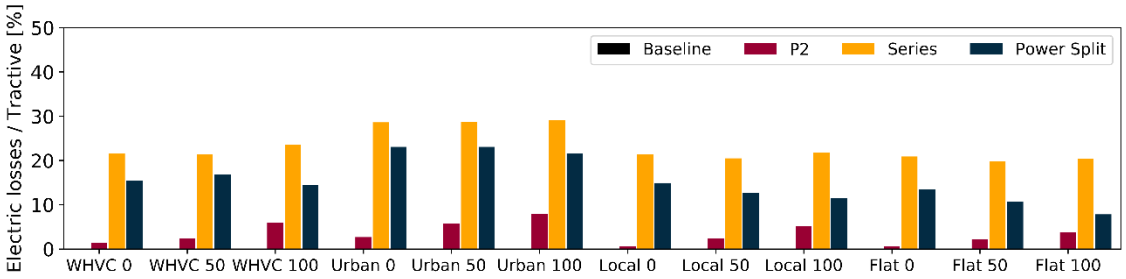

(c)

Figure 13. Engine average efficiency (a), percentage of energy recovery during braking with respect to the total tractive energy (b) and electric losses (c) for four driving cycles and three payload conditions.

To summarize the results, a spider graph with the main components selected and performance values is depicted in Figure 14. The performance results are the average value for the 12 driving conditions tested. In terms of components, the series and power split used the highest electric machines (the spider shows the total power of the traction motor and generator) and battery size. Specifically, the series, due to the separated ICE-wheels configuration, requires two large EM and the optimum battery size is 42 kWh, while the P2 only uses an EM seven times lower than the series and a battery size of only 8 kWh. The fuel energy save is similar for all the hybrids, consuming around 10% lower amount of fuel than the non-hybrid version. Similar behaviour is seen for the tailpipe CO_2 emissions. The other two main emissions that are wanted to be reduced using RCCI combustion are the NOx and soot. All the hybrid versions promote engine-out emissions levels under the EU VI normative (NOx<0.4 g/kWh and soot <10 mg/kWh). To have a complete vision of the powertrain potential, the dual-fuel dual-mode combustion (DMDF) non-hybrid case is also added. A complete description of the model can be seen in [20]. This concept uses the same operative condition than the RCCI ICE and changes to a more diffusive combustion in the range 210 hp to 280 hp. The DMDF allows reaching the NOx limit. However, due to the diffusive operation zone at high load, the average engine-out soot for all the DMDF conditions is 15 mg/kWh, out of the EU VI limit. Therefore, the hybrid powertrain allows to use the RCCI map with almost negligible soot emissions. This allows to remove (or at least to simplify) the particle filter device, reducing the aftertreatment system costs.

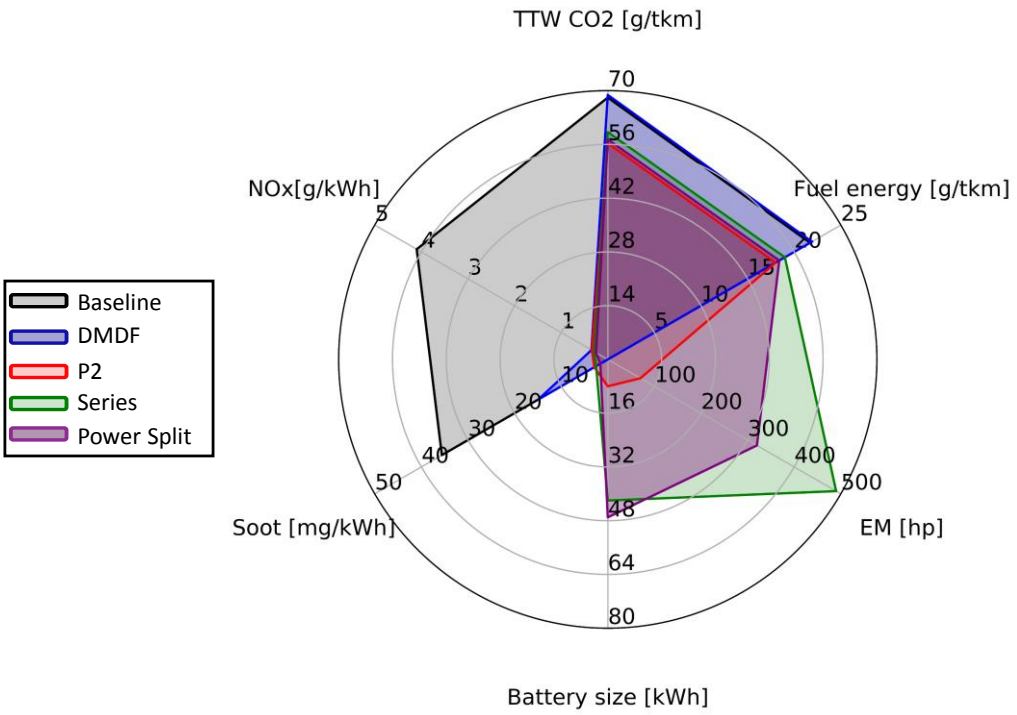

Figure 14. Spider graph resume for the results average under 4 driving cycles and 3 payload conditions.

One important point is the amount of gasoline used in the combustion concept with respect to the diesel amount. This is evaluated by means of the gasoline fraction (GF). When the GF is higher than 50%, it means that more gasoline than diesel is used in the driving cycle. Figure 15 shows that the P2 is the hybrid powertrain with the lowest GF due to the transient operation in the low load zone of the map (lowest GF, see Figure 1). For the P2, the GF only overpass the 50% in full payload conditions. The Series and Power Split used more gasoline than diesel, with an average around 75%. This result suggests that if a renewable fuel is used in the low reactivity port, the hybrid powertrain can help to large well-to-wheel CO_2 reduction. Synthetic gasoline is a potential e-fuel due to the renewable pathway in the fuel production.

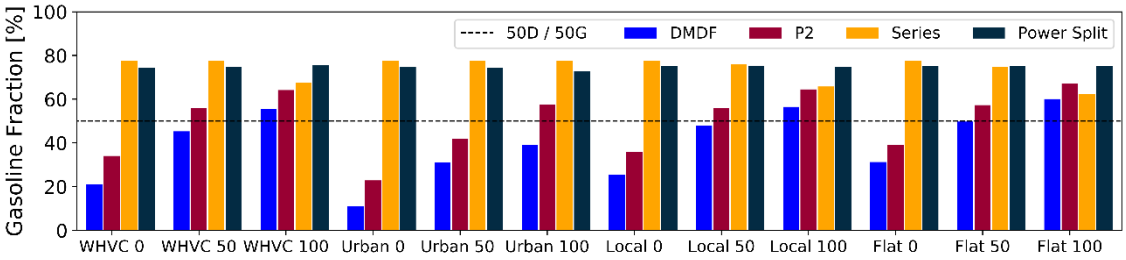

Figure 15. Gasoline fraction for four driving cycles and three payload conditions.

A final summary of the performance results at homologation conditions (WHVC at 50% payload) is included in Table 5. To study the potential of using a e-fuel, a calculation using the synthetic gasoline production values as substitute of the LRF (conventional gasoline) is performed. The main hypothesis is the assumption of equal characteristics between both fuels. In spite of that this needs to be tested in an

experimental test bench, it is a reasonable boundary condition following the works [40][41]. Considering the calibration maps shown in Figure 1, it can be inferred that the assumption of using synthetic gasoline will have a strong impact on the WTW CO_2 emissions in this combustion concept. In this sense, as the gasoline fraction is high, it is possible to achieve between 40% and 75% of WTW CO_2 reduction. It is important to remark that due to the reduced TTW CO_2 emissions and that the operation is concentrated at high loads for all the hybrids, these architectures achieve larger CO_2 reductions than the non-hybrid platforms. The P2 with synthetic gasoline provides the worst WTW results between the three hybrid configurations because it mainly uses the low load zone of the engine map. However, the final benefits of WTW CO_2 emissions are above 60% with respect to CDC.

Table 5. Summary results in homologation conditions (WHVC and 50% payload) including WTW CO_2 analysis.

Parameter	Non-hybrid		P2	Series	Power Split
Case	CDC	DMDF	RCCI	RCCI	RCCI
BSFC	236 g/kWh	+0.9%	-16.5%	-9.4%	-10.6%
BSNOx	3.9 g/kWh	-91%	-91%	-92%	-92%
BSsoot	36 mg/kWh	-93%	-93%	-95%	-92%
BSHC	0.11 g/kWh	+2882%	+2791%	+2127%	+1744%
BSCO	0.47 g/kWh	+1567%	+1228%	+786%	+917%
CO_2 TTW	59 g/tkm	-0.2%	-17.6%	-11.2%	-12.3%
CO_2 WTW	74 g/tkm	-0.7%	-18.1%	-12.0%	-12.5%
CO_2 WTW synthetic gasoline		-43.5%	-61.7%	-77.4%	-76.7%

4. Conclusion

This investigation analyzed the potential of different hybrid architectures representative of the European medium-duty truck sector. The ICE was calibrated in RCCI combustion mode with the target to reduce the ATS for NOx and soot. The results were compared to the OEM diesel truck. The components and control strategy optimization was done with a genetic algorithm at homologation conditions. The optimum powertrains were evaluated in 12 different conditions including several

payloads and real driving cycles. In addition, a WTW analysis was carried out for the optimum cases by replacing commercial gasoline with synthetic green gasoline. The main findings are summarized as follows:

- The hybrid configurations allow to achieve EU VI engine-out NOx and soot emissions without SCR and DPF for all the conditions by following a de-rating ICE strategy. The performance analysis shows higher wheel forces than the OEM truck. This goal was not achieved yet by any other combustion technology in a heavy-duty truck.
- The hybrid platforms allow to achieve from 12% (series and power split) to 16% (P2) of tailpipe CO_2 reduction with respect to the CDC non-hybrid case. These results are closer or even higher than the 2025 European target for the heavy-duty sector.
- The use of higher electric machine for series and power split not shows large advantages than in the P2 for the conditions tested. The extra regenerative braking between 70 hp and 280 hp of electric machine is limited.
- The HC and CO emissions are the main drawback of this technology. Dedicated oxidation catalyst analysis needs to be performed to see the effectiveness with high emissions rates and low exhaust temperatures.
- The series and power split use the highest gasoline fraction amount due to the almost stationary ICE operation. Using an e-fuel, as a synthetic gasoline, it is possible to achieve from 60% to 75% of CO_2 WTW saving with respect to CDC in homologation conditions (WHVC at 50% payload). In the case of the DMDF non-hybrid, it can achieve 43% of WTW CO_2 saving against CDC.

5. Acknowledgments

The authors thanks ARAMCO Overseas Company and VOLVO Group Trucks Technology for supporting this research. The authors also acknowledge the Conselleria de Innovación, Universidades, Ciencia y Sociedad Digital de la Generalitat Valenciana for partially supporting this research through grant number GV/2020/017.

6. References

[1] A. Beji, K. Deboudt, S. Khardi, B. Muresan, and L. Lumière, “Determinants of rear-of-wheel and tire-road wear particle emissions by light-duty vehicles using on-road and test track experiments,” *Atmos. Pollut. Res.*, no. August, Dec. 2020.

[2] J. R. Serrano, A. García, J. Monsalve-Serrano, and S. Martínez-Boggio, “High efficiency two stroke opposed piston engine for plug-in hybrid electric vehicle applications: Evaluation under homologation and real driving conditions,” *Appl. Energy*, vol. 282, no. October 2020, p. 116078, Jan. 2021.

[3] R. Payri, J. D. La Morena, J. Monsalve-Serrano, F. C. Pesce, and A. Vassallo, “Impact of counter-bore nozzle on the combustion process and exhaust emissions for light-duty diesel engine application,” *Int. J. Engine Res.*, vol. 20, no. 1, pp. 46–57, 2019.

[4] K. Forrest, M. Mac Kinnon, B. Tarroja, and S. Samuelsen, “Estimating the technical feasibility of fuel cell and battery electric vehicles for the medium and heavy duty sectors in California,” *Appl. Energy*, vol. 276, no. April, p. 115439, 2020.

[5] J. Benajes, A. García, J. Monsalve-Serrano, and S. Martínez-Boggio, “Emissions reduction from passenger cars with RCCI plug-in hybrid electric vehicle technology,” *Appl. Therm. Eng.*, vol. 164, no. September 2019, p. 114430, Jan. 2020.

[6] S. Imtenan *et al.*, “Impact of low temperature combustion attaining strategies on diesel engine emissions for diesel and biodiesels : A review,” *Energy Convers. Manag.*, vol. 80, no. x, pp. 329–356, 2014.

[7] Z. Li *et al.*, “Control of intake boundary conditions for enabling clean combustion in variable engine conditions under intelligent charge compression ignition (ICCI) mode,” *Appl. Energy*, vol. 274, no. January, p. 115297, Sep. 2020.

[8] S. Molina, A. García, J. Monsalve-Serrano, and D. Estepa, “Miller cycle for improved efficiency, load range and emissions in a heavy-duty engine running under reactivity controlled compression ignition combustion,” *Appl. Therm. Eng.*, vol. 136, no. December 2017, pp. 161–168, 2018.

[9] V. B. Pedrozo, I. May, W. Guan, and H. Zhao, “High efficiency ethanol-diesel dual-fuel combustion: A comparison against conventional diesel combustion from low to full engine load,” *Fuel*, vol. 230, no. May, pp. 440–451, Oct. 2018.

[10] S. L. Kokjohn, R. M. Hanson, D. A. Splitter, and R. D. Reitz, “Experiments and Modeling of Dual-Fuel HCCI and PCCI Combustion Using In-Cylinder Fuel Blending,” *SAE Int. J. Engines*, vol. 2, no. 2, pp. 2009-01–2647, Nov. 2009.

[11] J. Benajes, B. Tormos, A. Garcia, and J. Monsalve-Serrano, “Impact of Spark Assistance and Multiple Injections on Gasoline PPC Light Load,” *SAE Int. J. Engines*, vol. 7, no. 4, pp. 2014-01–2669, Oct. 2014.

[12] S. Molina, A. García, J. Monsalve-Serrano, and D. Villalta, “Effects of fuel injection parameters on premixed charge compression ignition combustion and emission characteristics in a medium-duty compression ignition diesel engine,” *Int. J. Engine Res.*, vol. 0, no. 0, p. 146808741986701, Jul. 2019.

[13] J. Benajes, A. Garcia, J. Monsalve-Serrano, and S. Martinez, “CO 2 Well-to-Wheel Abatement with Plug-In Hybrid Electric Vehicles Running under Low Temperature Combustion Mode with Green Fuels,” in *SAE Technical Paper*, 2020.

[14] J. Benajes, A. García, J. Monsalve-Serrano, I. Balloul, and G. Pradel, “Evaluating the reactivity controlled compression ignition operating range limits in a high-compression ratio medium-duty diesel engine fueled with biodiesel and ethanol,” *Int. J. Engine Res.*, vol. 18, no. 1–2, pp. 66–80, Feb. 2017.

[15] H. Wei, F. Liu, J. Pan, Q. Gao, G. Shu, and M. Pan, “Experimental study on the effect of pre-ignition heat release on GCI engine combustion,” *Fuel*, vol. 262, no.

October 2019, p. 116562, 2020.

[16] J. Benajes, A. García, J. Monsalve-Serrano, and V. Boronat, “Dual-Fuel Combustion for Future Clean and Efficient Compression Ignition Engines,” *Appl. Sci.*, vol. 7, no. 1, p. 36, Dec. 2016.

[17] A. García, J. Monsalve-Serrano, D. Villalta, and R. Sari, “Octane number influence on combustion and performance parameters in a Dual-Mode Dual-Fuel engine,” *Fuel*, vol. 258, no. May, p. 116140, 2019.

[18] V. Bermúdez, A. García, D. Villalta, and L. Soto, “Assessment on the consequences of injection strategies on combustion process and particle size distributions in Euro VI medium-duty diesel engine,” *Int. J. Engine Res.*, vol. 21, no. 4, pp. 683–697, 2020.

[19] A. García, J. Monsalve-Serrano, D. Villalta, and R. Lago Sari, “Performance of a conventional diesel aftertreatment system used in a medium-duty multi-cylinder dual-mode dual-fuel engine,” *Energy Convers. Manag.*, vol. 184, 2019.

[20] A. García, J. Monsalve-Serrano, S. Martinez-Boggio, P. Gaillard, O. Poussin, and A. A. Amer, “Dual fuel combustion and hybrid electric powertrains as potential solution to achieve 2025 emissions targets in medium duty trucks sector,” *Energy Convers. Manag.*, vol. 224, no. June, p. 113320, Nov. 2020.

[21] F. Millo, L. Rolando, R. Fuso, and J. Zhao, “Development of a new hybrid bus for urban public transportation,” *Appl. Energy*, vol. 157, pp. 583–594, 2015.

[22] IVECO, “FULL HYBRID RANGE,” 2020. .

[23] S. Gan, D. Chrenko, A. Kéromnès, and L. Le Moyne, “Development of a Multi-Architecture and Multi-Application Hybrid Vehicle Design and Management Tool,” *Energies*, vol. 11, no. 11, p. 3185, 2018.

[24] J. Benajes, A. García, J. Monsalve-Serrano, and S. Martínez-Boggio, “Optimization of the parallel and mild hybrid vehicle platforms operating under conventional and advanced combustion modes,” *Energy Convers. Manag.*, vol. 190, no. February, pp. 73–90, Jun. 2019.

[25] B. Helgeson and J. Peter, “The role of electricity in decarbonizing European road transport – Development and assessment of an integrated multi-sectoral model,” *Appl. Energy*, vol. 262, no. February 2019, p. 114365, 2020.

[26] A. P. Vora *et al.*, “Design-space exploration of series plug-in hybrid electric vehicles for medium-duty truck applications in a total cost-of-ownership framework,” *Appl. Energy*, vol. 202, pp. 662–672, 2017.

[27] Y. Li, H. He, A. Khajepour, H. Wang, and J. Peng, “Energy management for a power-split hybrid electric bus via deep reinforcement learning with terrain information,” *Appl. Energy*, vol. 255, no. August, p. 113762, 2019.

[28] B. Zhang, J. Zhang, F. Xu, and T. Shen, “Optimal control of power-split hybrid electric powertrains with minimization of energy consumption,” *Appl. Energy*, vol. 266, no. October 2019, p. 114873, 2020.

[29] W. Zhuang *et al.*, “A survey of powertrain configuration studies on hybrid electric vehicles,” *Appl. Energy*, vol. 262, no. December 2019, p. 114553, 2020.

[30] A. Rouhani, H. Kord, and M. Mehrabi, “A comprehensive method for optimum sizing of hybrid energy systems using intelligence evolutionary algorithms,” *Indian J. Sci. Technol.*, vol. 6, no. 6, pp. 4702–4712, 2013.

[31] B. Xu *et al.*, “Parametric study on reinforcement learning optimized energy management strategy for a hybrid electric vehicle,” *Appl. Energy*, vol. 259, no. August 2019, p. 114200, 2020.

[32] J. Benajes, A. García, J. Monsalve-Serrano, and S. Martínez-Boggio, “Potential of using OMEx as substitute of diesel in the dual-fuel combustion mode to reduce the global CO2 emissions,” *Transp. Eng.*, vol. 1, no. January, p. 100001, Jun. 2020.

[33] A. Guille des Buttes, B. Jeanneret, A. Kéromnès, L. Le Moyne, and S. Pélissier, “Energy management strategy to reduce pollutant emissions during the catalyst light-off of parallel hybrid vehicles,” *Appl. Energy*, vol. 266, no. March, p. 114866, 2020.

[34] J. Kargul *et al.*, “Benchmarking a 2018 Toyota Camry 2.5-liter atkinson cycle engine with cooled-EGR,” *SAE Tech. Pap.*, vol. 2019-April, no. April, pp. 601–638, 2019.

[35] Y. He *et al.*, “Multiobjective component sizing of a hybrid ethanol-electric vehicle propulsion system,” *Appl. Energy*, vol. 266, no. March, 2020.

[36] C. Forgez, D. Vinh Do, G. Friedrich, M. Morcrette, and C. Delacourt, “Thermal modeling of a cylindrical LiFePO4/graphite lithium-ion battery,” *J. Power Sources*, vol. 195, no. 9, pp. 2961–2968, 2010.

[37] JSOL-Corporation, “Motor design tool Jmag international,” 2020. [Online]. Available: https://www.jmag-international.com/express/. [Accessed: 26-May-2020].

[38] K. Deb and H. Jain, “An evolutionary many-objective optimization algorithm using reference-point-based nondominated sorting approach, Part I: Solving problems with box constraints,” *IEEE Trans. Evol. Comput.*, vol. 18, no. 4, pp. 577–601, 2014.

[39] K. Naimah, B. R. Mardanie, L. M. Dwi, S. N. Adi, and Sulistiyanto, “A review of technology assessment of green gasoline processing,” *Energy Reports*, vol. 6, pp. 1641–1649, 2020.

[40] J. Szczygieł and M. Kułażyński, “Thermodynamic limitations of synthetic fuel production using carbon dioxide: A cleaner methanol-to-gasoline process,” *J. Clean. Prod.*, vol. 276, 2020.

[41] H. Er-Rbib, C. Bouallou, and F. Werkoff, “Production of synthetic gasoline and diesel fuel from dry reforming of methane,” *Energy Procedia*, vol. 29, pp. 156–165, 2012.